International Journal of Modern Physics E, Vol. 1, No. 1 (1992) 1–37

NUCLEAR PHYSICS OF DARK MATTER DETECTION

J. ENGEL and S. PITTEL
Bartol Research Institute, University of Delaware, Newark, Delaware 19716, USA

and

P. VOGEL
Physics Department, California Institute of Technology, Pasadena, CA 91125, USA

Received 12 March 1992

We describe the elastic scattering of weakly interacting dark matter particles from nuclei, with laboratory detection in mind. We focus on the lightest neutralino (a neutral fermion predicted by supersymmetry) as a likely candidate and discuss the physics needed to calculate its elastic scattering cross section and interpret experimental results. Particular emphasis is placed on a proper description of the structure of the proposed detector nuclei. We include a brief discussion of expected count rates in some detectors.

1. Introduction

Dark matter is a term that describes nonluminous material in galaxies, clusters of galaxies, and possibly on even larger scales. A considerable body of evidence points to its existence; in fact, dark matter is probably more abundant than the familiar baryonic matter in stars, dust and gas, i.e. in objects that are accessible to traditional astrophysical observation. In a metaphorical sense, the adjective "dark" represents our ignorance of nearly everything about the subject. Contemporary physics is challenged even by such basic questions as: What is the dark matter made of, how much is there, and is it the same on all scales?

In this review we describe some of the theoretical background relevant to terrestrial dark matter detection. In Sec. 2 we briefly review the evidence for dark matter, and then discuss candidates that have been proposed for the dark matter in our galaxy. We argue that a hypothetical neutral particle predicted by supersymmetry, the "lightest neutralino", is one of the few viable candidates. If they indeed exist in the right abundance, neutralinos may be observable through elastic scattering from detector nuclei. In order to plan experiments and eventually interpret their results, however, we need to model neutralino–nucleus cross sections as accurately as possible. This requires first determining how neutralinos interact with nucleons, an endeavor in "particle physics", and then folding in the structure of the target nucleus. In Sec. 3, we discuss the relevant particle physics, first describing the supersymmetric theories that give rise to the neutralino hypothesis and then dis-

cussing the fundamental interactions of neutralinos with quarks and subsequently with nucleons. To set the stage for the detailed nuclear physics discussion to follow, we then present in Sec. 4 the formalism necessary to calculate elastic neutralino scattering cross sections from detector nuclei.

Sections 5 and 6 contain the main topic of our paper, the nuclear structure physics required for a description of neutralino elastic scattering. The interaction of neutralinos with matter can be classified according to two currents: scalar and axial vector. The cross sections that arise from the scalar current are fairly straightforward for any target nucleus and are discussed in Sec. 5. The cross sections from the axial current, on the other hand, require more detailed nuclear structure information. In Sec. 6, we describe the various methods that have been applied so far to this problem. These include both phenomenological methods, which provide information on the nuclear response only at low momentum transfer, and more microscopic treatments that also yield the finite momentum response. To date, calculations have been carried out for several viable detector nuclei, the most notable exception being ^{73}Ge, which we discuss briefly. We then conclude in Sec. 7 by presenting examples of expected count rates in some of the proposed detectors.

The subject of dark matter detection has been reviewed several times previously, most recently in Refs. 1, 2 and 3. Numerous conferences and workshops have also addressed particular aspects of the subject and the interested reader can find additional information in recent proceedings.[4] To our knowledge, however, none of the earlier reviews covers the nuclear physics of the problem in any detail.

2. Preliminaries on Dark Matter

2.1. *Evidence for dark matter*

It is customary to express the amount of matter of the universe in terms of the ratio $\Omega = \rho/\rho_0$, where ρ is the average density and ρ_0 is the critical density that separates models in which the universe expands forever ($\rho < \rho_0$) from those in which it ultimately recollapses ($\rho > \rho_0$). The critical density is related to the present value of the Hubble parameter H_0 by $\rho_0 = 3H_0/8\pi G_N$.

Purely theoretical arguments are often invoked in support of the value $\Omega = 1$ for which the universe is barely open. These are based in large part on "naturalness", realized appealingly in the inflation hypothesis. It is important to bear in mind, however, that theoretical prejudice is by no means essential to the conclusion that dark matter exists and is indeed prevalent in the universe.

Figure 1 reviews the empirical situation[2,5] with regards to Ω. It includes information from many different observations at a variety of scales. The total luminous matter observed in galaxies (in stars, gas, and dust) accounts for only about 1% of the critical density. Since the luminous matter is composed primarily of baryons, these observations provide a lower limit on the total amount of baryonic matter in the universe, labeled Ω_B in the figure.

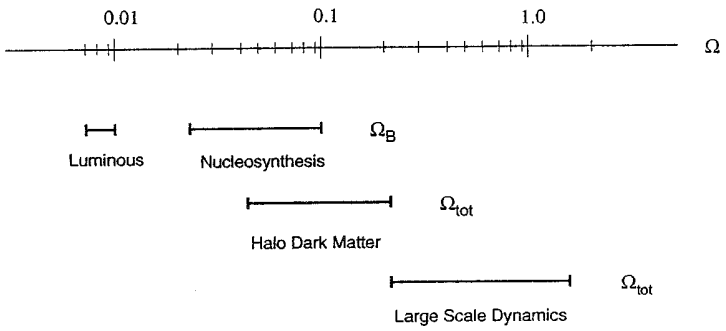

Fig. 1. Estimates of total density Ω and baryonic component Ω_B.

An independent estimate of Ω_B is provided by considering primordial nucleosynthesis. Combining relative-abundance measurements for the very light nuclei ^{2}H ^{3}He, ^{4}He and ^{7}Li with calculations of the synthesis of these nuclei shortly after the big bang,[6] one can roughly determine the overall photon to baryon ratio in the universe and therefore Ω_B. By comparing these estimates with those for luminous baryonic matter, we can conclude that (most likely) not all of the baryons in the universe are shining, i.e. some baryonic dark matter exists.

Dark matter, whether baryonic or nonbaryonic, manifests itself through its gravitational effects on nearby luminous matter. Results for the total matter densities at galactic and larger scales are summarized in the remaining two entries of the figure, labeled $\Omega_{\rm tot}$. Evidence on very large scales, most notably from the IRAS survey, suggests values for the total density that are consistent with $\Omega = 1$. Furthermore, this range of values for $\Omega_{\rm tot}$ indicates that at large enough scales nonbaryonic dark matter not only exists but actually predominates over baryons.

Since the discussion to follow will center around terrestrial detectors, our primary concern is dark matter within our own galaxy. Indeed, the evidence for galactic dark matter is particularly compeling. Figure 2 (Ref. 7) shows a "rotation curve" — a plot of velocity versus distance from the galactic center for luminous objects in a sample spiral galaxy. The velocities are obtained from red–shift analyses of e.g. the 21 cm hydrogen line. The figure also shows the curve that would obtain if the luminous matter alone were responsible for the gravitational forces. Beyond the edge of the galaxy, where only a few scattered luminous objects exist, this curve falls off roughly like $r^{-1/2}$. The actual curve shows no sign of such a drop, implying that the mass distribution extends well beyond the light distribution. In fact, of the many measured rotation curves, none displays any discernible falloff. It follows that at least 70–90% of the matter within galaxies is dark. Additional evidence, albeit weaker, suggests that these dark "halos" are roughly spherical in shape, with densities that eventually fall off as $1/r^2$. The constraints in Fig. 1 do not yet allow us to decide conclusively whether some or all of the halo dark matter is baryonic.

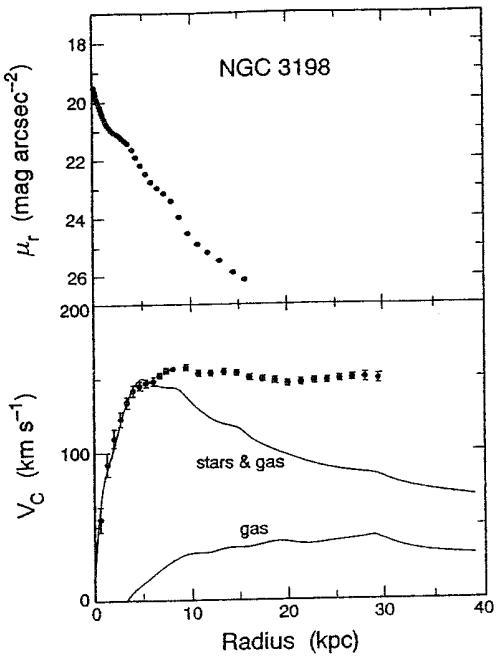

Fig. 2. Example of a rotation curve. The upper part shows the luminosity distribution for the galaxy NGC 3198. In the lower part the dots with error bars are the observed velocities. The predicted rotation curves based on the star and hydrogen gas distribution, are shown also. (Adopted from Ref. 7).

Whatever its composition, the dark matter's kinematics in our own galaxy are determined entirely by gravitational binding. Rotational velocities have been measured to about three times the distance between the center of the galaxy and the sun, implying that inside that distance (≈ 20 kpc) the dark halo contributes roughly three times more mass than the luminous material. The local halo density, obtained by extrapolation from larger distances,[2] is $\rho_{\rm halo} \approx 6 \times 10^{25}$ g cm^{-3} or 0.4 GeV cm^{-3}. If the halo is flattened somewhat, its density could be larger by a factor of about 1.5. The halo constituents are usually assumed to have a spherically symmetric Maxwellian distribution of velocities (cut off at some point), with $v_{\rm rms} \approx 270$ km s^{-1} $\approx 10^{-3}c$. By comparison, the sun moves in the galactic coordinate system with a velocity in the range 220–250 km s^{-1} and the earth orbits the sun at about 30 km s^{-1}. As we shall see shortly, the dark matter's kinematics constrain strategies for detecting and identifying it.

2.2. *Candidates for galactic dark matter*

As we have already noted, the dark matter in our galaxy could be composed entirely of baryons. However most ordinary objects, such as clouds of gas or dust, emit some form of radiation and are therefore not dark. Baryonic dark matter can only exist

as Massive Astrophysical Compact Halo Objects (MACHOs[8]), a generic category that includes large planets, brown dwarfs and black holes.

MACHOs can be detected through the characteristic brightening of stars directly behind them caused by gravitational microlensing.[9] Experiments to look for the time-dependent brightening of a great number of stars in the Large Magellanic Cloud[10,11] are currently under development. Obviously, if MACHOs are found — results from the first MACHO searches are expected in $\approx$1993 — the prospects for nonbaryonic galactic dark matter will be diminished. For now, however, in the absence of data, it is difficult to understand how enough MACHOs could be formed to account for all the dark matter and why they would be distributed spherically in halos. We shall assume from now on, therefore, that the halo dark matter is nonbaryonic and exists as elementary particles. Before discussing specific candidates, we need to touch briefly on the evolution of particle densities in the early universe.

Most candidates fall under the rubric "thermal relics". These are massive particles that were in thermal equilibrium at cosmologically early times (when the temperature T was high) in numbers comparable to that of the photon. As the universe cooled, the abundance tracked equilibrium values until the "freeze out" temperature T_F, when the particle interaction rate dropped below the expansion rate of the universe.[12] At that point annihilation ceased and thereafter the number of particles per comoving volume did not change from its equilibrium value at T_F. The present abundance of a thermal–relic species is therefore completely specified by its mass and annihilation cross section.

Roughly speaking, thermal relics can be further subdivided into two classes — hot and cold. Hot relics were relativistic at freeze out and exist with present number densities, comparable to that of photons, that are essentially independent of the value of T_F. A light neutrino ($m \leq 1$ MeV) is perhaps the most attractive hot–relic candidate. A neutrino of mass m_ν (in eV) would today contribute to Ω an amount[12]

$$\Omega_\nu = m_\nu/(23h_{50}^2) \ , \tag{2.1}$$

where h_{50} is the Hubble parameter in units of 50 km s^{-1} and is generally believed to lie in the range $0.8 \leq h_{50} \leq 1.3$. Light neutrinos of mass 10–50 eV could therefore provide a significant fraction of the critical density. Unfortunately, other considerations make it difficult to believe that galactic halos consist of light neutrinos. The Pauli principle limits the number of light fermions that can be packed into a space the size of a galaxy. Furthermore, all hot relativistic relics, neutrinos included, tend to erase galaxy-sized density fluctuations in the early universe, making the formation of galaxies a difficult proposition. While neither of these arguments is conclusive, they do weigh against hot dark matter.

Cold relics, on the other hand, were already nonrelativistic by the time of freeze out, usually because they are much heavier, and are considerably less abundant today than photons. The sparse, heavy, slow-moving particles are not vulnerable to either of the objections above.

Coincidentally, if a particle weighing a few GeV is to provide the critical density its annihilation cross section must be on the order of 10^{-37} cm^2, close to typical weak-interaction values. Heavy neutrinos are the most obvious cold relic candidates. None of the three known neutrinos is heavy, however, and the SLC/LEP measurements[13] of the width of Z^0 preclude a fourth generation. A more viable cold relic candidate — the object of our focus from now on — is the lightest neutralino, a hypothetical particle predicted by supersymmetry. We shall describe the properties of neutralinos in the next section. Here we stress only that they are stable and that their mass and annihilation cross sections completely determine their present density. Since neutralino masses and couplings are designed to lie near the weak scale, their relic densities are significant no matter what the details of the supersymmetry model.

We will not discuss nonthermal relics in this review. Before moving on though, we should note that a particle from this class — the axion — is one of the more appealing dark matter candidates. Most of axion parameter space has already been ruled out but a window remains for dark-matter axions of mass 10^{-6} eV $\leq m_a \leq 10^{-3}$ eV. Even though they are very light, a considerable fraction of such axions would be nonrelativistic or cold and thus consistent with the requirements of galaxy formation. Some experiments to detect these light bosons are underway but are not yet conclusive. For information and further references on axions, see the book of Kolb and Turner.[12]

3. Neutralinos and their Interactions

3.1. *Supersymmetry and neutralinos*

Neutralinos are considered good dark matter candidates partly because the theories that predict them were invented to address shortcomings in the Standard Model, without attention to the issue of dark matter; the link was only made later.[14,15] The Standard Model is commonly assumed to be the low energy limit of some more fundamental theory that applies at or before the Planck scale $M_P = (\hbar c/G_N)^{1/2} = 1.22 \times 10^{19}$ GeV. Radiative corrections tend to give the Higgs boson a mass at this very large scale; keeping the physical Higgs much lighter requires an awkward fine-tuning of parameters in the more fundamental Lagrangian at each order of perturbation theory. Supersymmetry ameliorates this "hierarchy problem" by introducing a partner with equal mass but opposite statistics for every particle in the Standard Model. Quadratic divergences in the Higgs propagator are then canceled exactly by contributions from the new particles. The symmetry is obviously slightly broken in the real world, but for the scheme to solve the hierarchy problem the new particles must have masses at roughly the weak scale. If supersymmetry is not seen below 1–10 TeV, its appeal largely disappears.

With this accepted, the neutral color-singlet superparticles become natural candidates for dark matter. In the minimal supersymmetric extension of the Standard Model, there are only a few of these objects: sneutrinos (the scalar partners of

neutrinos) and neutralinos, the spin 1/2 partners of the colorless gauge and Higgs bosons. For technical reasons, supersymmetric theories must include two Higgs doublets, responsible separately for the masses of the up- and down-type quarks, and thus there are at least 4 neutralinos: the W-ino ($\widetilde{W}_3$), the B-ino ($\widetilde{B}$), and two Higgsinos ($\widetilde{H}_1$ and $\widetilde{H}_2$). The sneutrino carries vector current and as a result interacts strongly enough with heavy nuclei to be ruled out as the halo dark matter by existing experiments.[1] Neutralinos are Majorana fermions and as a consequence carry no vector current, a fact that (as we shall see) severely limits the strength of their interactions with ordinary matter.

To be a significant component of the dark matter, the lightest neutralino — a linear combination of the 4 objects above — must be stable. In many supersymmetric models, this is insured (provided all "charginos" are heavier) by the conservation of a multiplicative quantum number called R-parity[16] that is given for any particle with spin s, baryon number B, and lepton number L by $R = (-1)^{2s+3B+L}$. A single neutralino has $R = -1$ and cannot decay entirely into ordinary particles, all of which have $R = 1$.

In the simplest models, the particular linear combination that defines the lightest neutralino follows from the values of four parameters in the superlagrangian (we adopt with minor modifications the notation of Ref. 16). Two of these, called M and M', specify the strength of supersymmetry breaking terms. A third, $\tan\theta_v$, is given by the ratio of vacuum expectation values of the two Higgs scalars, and the final parameter μ is a Higgsino mass. The overall neutralino mass term can be written as $-\frac{1}{2}\psi^T Y \psi$, where

$$\psi = (\widetilde{W}_3, \widetilde{B}, \widetilde{H}_1, \widetilde{H}_2) \tag{3.2}$$

and

$$Y = \begin{pmatrix} M' & 0 & -M_Z \cos\theta_v \sin\theta_W & M_Z \sin\theta_v \sin\theta_W \\ 0 & M & M_Z \cos\theta_v \cos\theta_W & M_Z \sin\theta_v \cos\theta_W \\ -M_Z \cos\theta_v \sin\theta_W & M_Z \cos\theta_v \cos\theta_W & 0 & -\mu \\ M_Z \sin\theta_v \sin\theta_W & -M_Z \sin\theta_v \cos\theta_W & -\mu & 0 \end{pmatrix} . \tag{3.3}$$

Here M_Z is the Z mass and θ_W is the Weinberg angle. We will denote the lowest-energy eigenvector of the matrix Y by

$$\chi = Z_1\widetilde{B} + Z_2\widetilde{W}_3 + Z_3\widetilde{H}_1 + Z_4\widetilde{H}_2 \ . \tag{3.4}$$

If the theory is embedded in a simple Grand-Unified group, the parameters M and M' are related by $M' = \frac{5}{3}M\tan^2\theta_W$. In the canonical model, then, only three parameters completely determine the structure and mass of the lightest neutralino. Figure 3 shows the neutralino mass and composition for a wide range of μ and M at a fixed value of $\tan\theta_v = 8$. In most of the available parameter space, particularly if the neutralinos are heavier than 50–100 GeV, the lightest neutralino turns out[17]

to be either a nearly pure $\widetilde{B}$ or a nearly symmetric (or antisymmetric) combination of $\widetilde{H}_1$ and $\widetilde{H}_2$. This point is important because recent experiments[18] at LEP have significantly reduced the chances that neutralinos are lighter than the Z.

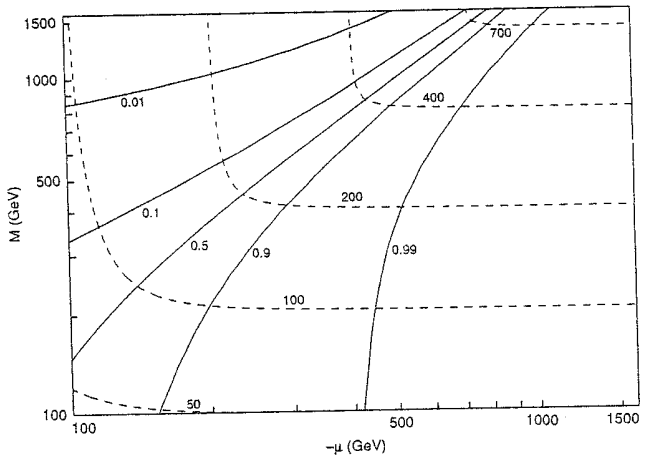

Fig. 3. Neutralino mass and composition versus μ and M. The dashed lines are contours of constant mass M_χ in GeV, and the solid lines are contours of constant "gaugino fraction" $(Z_1^2 + Z_2^2)$.

3.2. *Neutralino interactions*

Neutralinos interact with ordinary matter via diagrams of the type shown in Fig. 4; the intermediate particles can be normal gauge bosons, Higgs bosons, or squarks. These diagrams determine not only the scattering of halo neutralinos from ordinary matter, which we discuss in detail below, but also (in part) the annihilation rates of neutralinos in the early universe. One reason neutralinos make attractive dark-matter candidates, as mentioned previously, is that for a wide range of supersymmetry parameters their residual abundance after freezing out of equilibrium is consistent with $\Omega \simeq 1$.

The diagrams in Fig. 4, once evaluated (see Ref. 16), result in a low-momentum-transfer effective neutralino–quark Lagrangian density of the form

$$\mathcal{L} = \frac{g^2}{2M_W^2} \sum_q \left(\overline{\chi}\gamma^\mu\gamma_5\chi \; \overline{\psi}_q\gamma_\mu[V_q + A_q\gamma_5]\psi_q + \overline{\chi}\chi \; S_q \frac{m_q}{M_W} \overline{\psi}_q\psi_q + \overline{\chi}\gamma_5\chi P_q \; \overline{\psi}_q\gamma_5\psi_q \right). \tag{3.5}$$

The quark axial-vector and scalar current coefficients are given by[19,20]

$$A_q = \frac{1}{2} T_{3q}(Z_3^2 - Z_4^2) - \frac{M_W^2}{M_q^2} \left(\left[T_{3q} Z_2 - \tan\theta_W (T_{3q} - e_q) Z_1 \right]^2 + \tan^2\theta_W e_q^2 Z_1^2 + \frac{2m_q^2 d_q^2}{4M_W^2} \right),$$

$$S_q = \frac{1}{2}(Z_2 - \tan\theta_W Z_1)\left[\frac{M_W^2}{M_{H_2}^2} g_{H_2} k_q^{(2)} + \frac{M_W^2}{M_{H_1}^2} g_{H_1} k_q^{(1)} + \frac{\epsilon d_q M_W^2}{M_{\tilde{q}}^2}\right], \tag{3.6}$$

where $\tilde{q}$ is a squark (the scalar partner of a quark); T_{3q} is weak isospin; e_q is the charge; $d_q = Z_4/\sin\theta_v$, $k_q^{(1)} = \sin\alpha/\sin\theta_v$, and $k_q^{(2)} = \cos\alpha/\sin\theta_v$ for up-type quarks (α is an angular function of the Higgs masses specified in Ref. 21); $d_q = -Z_3/\cos\theta_v$, $k_q^{(1)} = \cos\alpha/\cos\theta_v$, and $k_q^{(2)} = -\sin\alpha/\cos\theta_v$ for down-type quarks; $g_{H_2} = Z_3\sin\alpha + Z_4\cos\alpha$; $g_{H_1} = Z_3\cos\alpha + Z_4\sin\alpha$ (H_2 and H_1 are the lightest and heaviest neutral Higgs scalars respectively); and ϵ is the sign of the lightest-neutralino mass eigenvalue. We do not give expressions for V_q and P_q because, as we show below, they contribute negligibly to scattering in the nonrelativistic limit. As is clear from Eq. (3.6), the effective axial-vector current results from Z and squark exchange, while the scalar current is due to Higgs and squark exchange. The strengths of the interactions depend on the masses of these exchanged particles, as well as on the coefficients Z_i that specify the composition of the lightest neutralino.

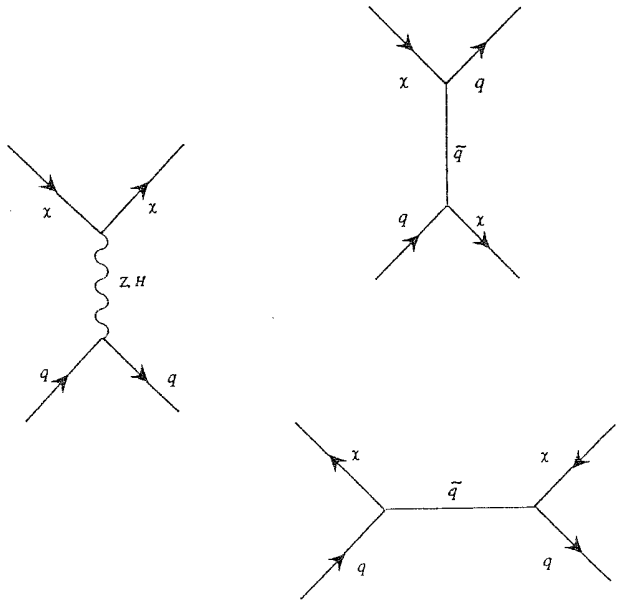

Fig. 4. Feynman diagrams describing neutralino–quark scattering.

3.3. *Effective interaction of neutralinos with nucleons*

Because the galactic neutralinos move so slowly ($\overline{v} \simeq 10^{-3}c$), the time component of their axial current can be neglected compared to the space components. Thus, at the

nucleon level, only the space components of the hadronic current need be considered. But the space components of the nucleonic vector current are suppressed compared to those of the axial current by factors of $v_N/c \simeq 0.1$, (N stands for nucleon) or $q/M_N c$ (q is the momentum transfer), which as we will discuss shortly, must also be small except in very heavy nuclei. The vector interaction can therefore be neglected, as, for similar reasons, can the pseudoscalar interaction.

As a consequence, we can write the effective Lagrangian for the interaction of nucleons with neutralinos in the form

$$L = \frac{g^2}{2M_W^2} \int d^4x \left[\overline{\chi}\gamma^\mu\gamma_5\chi \; \mathcal{J}_\mu^5(x) + \overline{\chi}\chi \mathcal{S}(x) \right] , \tag{3.7}$$

where

$$\mathcal{J}_\mu^5(x) = \sum_q A_q \overline{\psi}_q(x)\gamma_\mu\gamma_5\psi_q(x) \tag{3.8}$$

and

$$\mathcal{S}(x) = \sum_a S_q \frac{m_q}{M_W} \overline{\psi}_q(x)\psi_q(x) , \tag{3.9}$$

are the axial-vector and scalar hadronic currents, respectively. Our next task is to evaluate the nuclear matrix elements of these objects.

We will make the usual assumption that a nucleus is just a collection of interacting nucleons, so that the nuclear matrix element of any current operator can be obtained from its one-nucleon matrix element and a nuclear wave function. Since the axial-vector and scalar currents do not interfere in the cross section, we can consider each independently.

With some further quite reasonable assumptions described below, the one-nucleon axial-current matrix elements $\langle [N]p,s|\, \mathcal{J}_\mu^5(x)\, |[N]p',s'\rangle$, where p and p' are on-shell four momenta and s and s' are spin labels, can be extracted from experimental data. Lorentz invariance and the requirement that second class currents are absent restrict the matrix element to the form

$$\begin{aligned} \langle [N]p,s|\, \mathcal{J}_\mu^5(x)\, |[N]p',s'\rangle \;&=\; \overline{U}_N(p,s)\frac{1}{2}\left[(a_0 + a_1\tau_3)\gamma_\mu\gamma_5 + (b_0 + b_1\tau_3)q_\mu\gamma_5\right] \\ &\quad \times U_N(p',s')e^{iq^\nu x_\nu} , \end{aligned} \tag{3.10}$$

where U_N is a nucleon spinor, $q_\mu = (p-p')_\mu$ and a_0, b_0 and a_1, b_1 are isoscalar and isovector coefficients, respectively. At $q = 0$, the second term drops out and the a's are completely determined by the A_q and three numbers Δq (for $q = u$, d and s quarks) defined by

$$\Delta q s^\mu = \langle p,s|\, \overline{\psi}_q\gamma^\mu\gamma_5\psi_q\, |p,s\rangle , \tag{3.11}$$

where the matrix element is for the proton, and s^μ is the spin vector defined in the usual way.[22] Specifically,

$$\begin{aligned} a_0 &= (A_u + A_d)(\Delta u + \Delta d) + 2A_s\Delta s , \\ a_1 &= (A_u - A_d)(\Delta u - \Delta d) . \end{aligned} \tag{3.12}$$

The Δq represent the fractional spin of the proton carried by quarks of type q. Assuming flavor SU(3) symmetry, one can extract two independent combinations of the three Δq, denoted by F and D, from the observed semileptonic decay rates of baryons in the lowest octet (the axial coupling constant of the neutron, g_A, is represented in this scheme by $F + D$). Fits to all the decays indicate that SU(3) symmetry for the axial current operators is in fact reasonably good [22] and fix F and D at

$$\begin{aligned} F &= 1/2(\Delta u - \Delta s) = 0.47 \pm 0.04 \ , \\ D &= 1/2(\Delta u - 2\Delta d + \Delta s) = 0.81 \pm 0.03 \ . \end{aligned} \tag{3.13}$$

A third combination, $(1/9)(4\Delta u + \Delta d + \Delta s) = 0.175 \pm 0.018$, has been measured in polarized electron and muon scattering experiments,[23,24] but here the results must be regarded with a little caution. The measurements were actually made at a momentum transfer in or near the scaling regime; the assumption that the result does not change significantly below $Q^2 = 1$ GeV^2, when the strong interaction becomes strong, has not been completely proved. Taken along with the above values for F and D, the EMC muon measurement implies

$$\begin{aligned} \Delta u &= 0.78 \pm 0.08 \ , \\ \Delta d &= -0.50 \pm 0.08 \ , \\ \Delta s &= -0.16 \pm 0.08 \ . \end{aligned} \tag{3.14}$$

The nonnegligible value for the strange quark matrix element has aroused considerable attention, as has the fact that the three numbers sum almost to 0, implying that gluons carry all the proton's spin. The conventional nonrelativistic constituent quark model (that identifies quarks as QCD partons) predicts instead $\Delta u = 0.97$, $\Delta d = -0.28$, $\Delta s = 0$, though with reasonable modifications [25,26] the model can be made consistent with the EMC data. We will use the numbers in Eq. (3.14) as best estimates based on current knowledge.

The b coefficients can be estimated from PCAC, just as they are for the axial weak current; the second term is induced by the exchange of virtual mesons. The isoscalar mesons are heavy enough to set $b_0 \approx 0$ and pion exchange induces an isovector coefficient

$$b_1 = \frac{m_N a_1}{|\mathbf{q}|^2 + m_\pi^2} \ , \tag{3.15}$$

where m_N is the nucleon mass, q_0 has been assumed to be small and an analog of the Goldberger–Triemann relation has been used. The b_1 term contributes significantly to the scattering for $q \gtrsim m_\pi$.

Turning now to the scalar interaction, we note that the coefficients S_q are multiplied by m_q/M_W. Since the proton is constructed nominally from up and down quarks, which are light compared to the W, the scalar term would seem to contribute negligibly. This conclusion is too hasty, however, for several reasons. The

strength of the coupling is determined by the nucleon matrix elements of the scalar current

$$\langle [N]p,s|\,\mathcal{S}(x)\,|[N]p',s\rangle = \overline{U}_N(p,s)(c_0+c_1\tau_3)U_N(p',s)e^{iq^\nu x_\nu}\ , \tag{3.16}$$

where the coefficients c_0 and c_1 are functions of the S_q in Eq. (3.6) and several new numbers λ_q defined by

$$\lambda_q = \langle p,s|\,\frac{m_q}{M_W}\overline{\psi}_q\psi_q\,|p,s\rangle\ . \tag{3.17}$$

From the measured "σ-term" in the pion–nucleon scattering amplitude and SU(3) considerations,[27] it follows that strange quarks are substantially present in the proton, viz.

$$\lambda_s \simeq 0.0017\ . \tag{3.18}$$

Furthermore,[28] each flavor of heavy quark contributes an effective matrix element

$$\lambda_h \simeq 0.0005\ . \tag{3.19}$$

The quantities λ_s and λ_h are still fairly uncertain; we neglect the consistency requirement between them as well as the small contribution from up and down quarks.[29] Assuming the strange (and heavy) matrix elements are equal in the proton and neutron, the isospin structure of the scalar current is

$$\begin{aligned} c_0 &= S_s\lambda_s + \sum_h S_h\lambda_h\ , \\ c_1 &= 0\ . \end{aligned} \tag{3.20}$$

Though the coefficient c_0 is small, the scalar interaction is "constructively" coherent and the cross section for scattering from nuclei acquires a factor of A^2, where A is the number of nucleons. The scalar contribution can therefore be comparable to or larger than the axial-current cross section in heavy nuclei, particularly if one of the Higgs bosons is relatively light.

Before deriving scattering cross sections, let us look briefly at the nonrelativistic limit of the one-nucleon current matrix elements (an appropriate limit since the nucleon velocity is typically about $0.1c$). As mentioned, the time component of the axial vector current is irrelevant since it contracts with the very small time component of the neutralino current. For the spatial and scalar currents, we have, from Eqs. (3.9), (3.14), (3.15) and (3.19)

$$\begin{aligned} \langle [N]p,s|\,\mathcal{J}(x)\,|[N]p',s'\rangle &\longrightarrow \left\langle [N]s|\,\frac{1}{2}(a_0+a_1\tau_3)\boldsymbol{\sigma} - \frac{1}{2}\frac{\boldsymbol{\sigma}\cdot\mathbf{q}\,a_1\tau_3}{q^2+m_\pi^2}\,\mathbf{q}\,|[N]s'\right\rangle \\ &\qquad e^{-i(\mathbf{q}\cdot\mathbf{x}-wt)}\ , \\ \langle [N]p,s|\,\mathrm{S}(x)\,|[N]p',s'\rangle &\longrightarrow \delta_{s,s'}c_0e^{-i(\mathbf{q}\cdot\mathbf{x}-wt)}\ , \end{aligned} \tag{3.21}$$

where $|[N]s\rangle$ and $|[N]s'\rangle$ are nonrelativistic two-component spinors. The coefficients a_0, a_1 and c_0 vary in principle with q but we shall assume the variation is slow

enough to ignore. In the limit $q = 0$ the axial current is just the nucleon spin and the scalar current simply counts nucleons. The axial current therefore gives rise to "spin–dependent" scattering and the scalar current to "spin–independent" scattering. We will use the two sets of terminology interchangably from now on.

4. Neutralino Scattering from Nuclei

At present, two promising methods for detecting neutralinos are under development. The first is indirect, involving the detection of high-energy neutrinos from the sun[28] or the center of the earth.[30] The particles lose energy through collisions in the sun or earth and are trapped; subsequently they occasionally find one another and annihilate producing the neutrinos, muons from which can be observed in water Cerenkov detectors. Though these experiments are interesting, we will not discuss them here. The second method measures the effects of neutralino–nucleus collisions in detectors on earth. The neutralino kinetic energies are low enough so that most detectors will register only the nuclear recoil associated with elastic scattering. We note, however, that some authors have considered the possibility of inelastic excitation of low-energy nuclear states.[31] Their conclusions are generally pessimistic, largely because of reduced phase space, and we will restrict ourselves here to elastic processes.

In the elastic scattering of a projectile of mass M_χ off a target of mass M_A, the maximum momentum transfer to the target is $q_{\rm max} = 2M_R v$, where M_R is the reduced mass of the system and v is the laboratory velocity of the projectile. If the kinematically allowed momentum transfers are small compared to the inverse size of the nucleus, i.e. if $q_{\rm max} R << 1$, the projectile can only probe average nuclear properties. If, on the other hand, $q_{\rm max} R$ is of order unity or larger, details of the radial distribution of nucleons may be important. A simple set of rules summarizes these considerations. For neutralino velocities of order $10^{-3}c$, the quantity $q_{\rm max} R < 1$ provided that (i) $A < 28$ (for any mass neutralino) or (ii) $M_\chi < 100A/(1.2A^{4/3} + 100)$ GeV. One obvious implication is that finite q effects are never important in light nuclei. Early calculations of detector response to neutralinos were restricted to $q = 0$, where the only nuclear information of relevance, as we show shortly, is the total nuclear mass (for the scalar current) and the total proton and neutron spin (for the axial current). For heavy neutralinos the maximum momentum transfer is not necessarily small if $A \gtrsim 30$ and the issue of finite momentum transfer and the associated form factors must be addressed.

With the assumption that the nucleus is a collection of nucleons interacting via static potentials, it is straightforward to derive expressions for neutralino–nucleus scattering for all momentum transfer q. In the impulse approximation, we have

$$\frac{d\sigma}{dq^2} = \frac{G_F^2}{\pi(2J+1)v^2} \sum_{s,s',M,M'} \left[|\mathcal{M}_A|^2 + |\mathcal{M}_S|^2\right], \tag{4.22}$$

where J is the ground state angular momentum and

$$\mathcal{M}_A = \langle s|\,\sigma_\chi\,|s'\rangle \cdot \int d^3x\,\langle JM|\,\mathcal{J}(\mathbf{x})\,|JM'\rangle\,e^{i\mathbf{q}\cdot\mathbf{x}}\,,$$
$$\mathcal{M}_S = \delta_{s,s'}\int d^3x\,\langle JM|\,\mathcal{S}(\mathbf{x})\,|JM'\rangle\,e^{i\mathbf{q}\cdot\mathbf{x}}\,. \tag{4.23}$$

In the above, the currents $\mathcal{J}$ and $\mathcal{S}$ are understood to be the sums of objects with the one-nucleon matrix elements given in the previous section. The time variable has been integrated out to give overall energy conservation. To evaluate Eq. (4.22), we expand the currents in vector spherical harmonics

$$\frac{d\sigma}{dq^2} = \frac{8G_F^2}{(2J+1)v^2}\,[S_A(q)+S_S(q)]\,,$$
$$S_A(q) = \sum_{L\ odd}\left(|\langle J\|\mathcal{T}^{el5}_L(q)\|J\rangle|^2 + |\langle J\|\mathcal{L}^5_L(q)\|J\|J\rangle|^2\right), \tag{4.24}$$
$$S_S(q) = \sum_{L\ even}|\langle J\|\mathcal{C}_L(q)\|J\rangle|^2\,,$$

where $\mathcal{T}^{el5}(q)$ and $\mathcal{L}^5(q)$ are the transverse electric and longitudinal projections of the axial current, defined generally e.g. in Ref. 32 and $\mathcal{C}$ is the "Coulomb projection" (we have abused the notation somewhat because we are projecting from a scalar object rather than the time component of a four vector, as is more usual). In our context, these operators can be written in the explicit form

$$\mathcal{C}_L(q) = \sum_i c_0 j_L(qr_i)Y_L(\hat{r}_i)\,,$$
$$\mathcal{T}^{el5}_L(q) = \frac{1}{\sqrt{2L+1}}\sum_i\frac{1}{2}(a_0+a_1\tau_3^i)\left[-\sqrt{L}\mathbf{M}_{L,L+1}(q\mathbf{r}_i)+\sqrt{L+1}\mathbf{M}_{L,L-1}(q\mathbf{r}_i)\right],$$
$$\mathcal{L}^5_L(q) = \frac{1}{\sqrt{2L+1}}\sum_i\frac{1}{2}\left(a_0+\frac{a_1m_\pi^2\tau_3^i}{q^2+m_\pi^2}\right)\left[\sqrt{L+1}\mathbf{M}_{L,L+1}(q\mathbf{r}_i)+\sqrt{L}\mathbf{M}_{L,L-1}(q\mathbf{r}_i)\right], \tag{4.25}$$

where $\mathbf{M}_{L,L'}(q\mathbf{r}_i) = j_{L'}(qr_i)[Y_{L'}(\hat{r}_i)\boldsymbol{\sigma}_i]^L$ (the brackets indicate angular momentum coupling) and the sum is over individual nucleons i.

At $q=0$, the axial structure function S_A receives contributions only from $\mathbf{M}_{1,0}$ and reduces to the form

$$S_A(0) = \frac{1}{4\pi}\left|\left\langle J\right\|\sum_i\frac{1}{2}(a_0+a_1\tau_3^i)\boldsymbol{\sigma}_i\left\|J\right\rangle\right|^2, \tag{4.26}$$

or equivalently, in neutron–proton representation,

$$S_A(0) = \frac{1}{4\pi}|(a_0+a_1)\langle J\|\hat{S}_p\|J\rangle + (a_0-a_1)\langle J\|\hat{S}_n\|J\rangle|^2\,, \tag{4.27}$$

where $\hat{S}_p$ and $\hat{S}_n$ denote the total spin operators for protons and neutrons respectively. Since the individual nucleon spins tend to cancel, the reduced matrix

elements in Eq. (4.27) are typically of order unity. In the next section, we will estimate $S_A(0)$ by relating the total proton and neutron spins to measured magnetic moments and beta-decay lifetimes.

At higher q, unfortunately, the isovector and isoscalar amplitudes interfere and we have to express the structure function as

$$S_A(q) = a_0^2\ S_{00}(q) + a_1^2\ S_{11}(q) + a_0 a_1\ S_{01}(q)\ , \tag{4.28}$$

where the three functions $S_{00}(a)$, $S_{11}(q)$ and $S_{01}(q)$ can be worked out from Eq. (4.25). The interference and q-dependence make it difficult to extract the three functions from experimental data.

In the scalar structure function S_S, the dominant contribution is from the $L = 0$ multipole and we can neglect the rest. The term $\langle J \| \mathcal{C}_0 \| J \rangle$ can be modeled as the Fourier transform of a spherically symmetric density, e.g. a Gaussian,[33,34] or via a more sophisticated approximation. In the low q limit

$$S_S(0) = \frac{2J+1}{4\pi} c_0^2 A^2\ , \tag{4.29}$$

which, as we have noted, depends coherently on the total mass of the nucleus and therefore, despite the size of c_0, may exceed $S_A(0)$ in heavy nuclei. In fact, we should point out here that *in even–even nuclei spin–independent scattering is all that can occur*; the spin–dependent cross section vanishes identically in $J = 0$ ground states.

With all the relevant formalism now in hand, we are ready to examine a variety of prospective detector nuclei, with an eye to setting meaningful limits on dark matter flux. Currently dark matter searches are conducted with underground detectors designed originally for double-beta-decay experiments. While these measurements have ruled out certain dark matter candidates, they are not sensitive enough to detect neutralinos. However, several more sensitive detectors, sometimes involving newly developed cryogenic technology, have recently been proposed, and some are already under development. Among light nuclei, some of the most appealing candidates are ^{19}F and ^{29}Si. Fluorine is considered promising largely because (according to calculations) it should scatter neutralinos fairly strongly.[29] Silicon is the basis of a prototype cryogenic detector[35] and thus is also a natural candidate. Some heavier nuclei have been suggested as well. ^{131}Xe would constitute an important ingredient in a fairly conventional scintillation detector.[36] Both ^{93}Nb (Ref. 37) and ^{73} Ge(Ref. 38) have been discussed in the context of the new-technology cryogenic systems, and the development of a detector based in part on the latter is well underway.

5. Spin–Independent Neutralino Elastic Scattering

The cross section for elastic scattering through the scalar term is fairly straightforward, and simple methods can be applied in all nuclei. As noted above, the scalar

structure function can be written as

$$S_S(q) \approx |\langle J \| C_0(q) \| J \rangle|^2 \equiv S_S(0) F^2(q) \ , \tag{5.30}$$

where $F(q)$ is the (normalized) Fourier transform of a spherical nuclear ground state density distribution. Very accurate data on charge distributions have been obtained from elastic electron scattering. Information on mass distributions is not as precise, although significant advances in recent years have come through pion elastic scattering. For our purposes, we can assume that the charge and mass distributions are roughly proportional.

Most of the work on finite momentum transfer (often referred to as "loss of coherence") in the spin–independent cross section [33,34] has approximated the nuclear density distribution $\rho(r)$ by a Gaussian with mean-square radius $\sqrt{(3/5)}R$, with $R = 1.2A^{1/3}$ fm. The resulting form factor is

$$F_a(q) = e^{-\frac{1}{10}(qR)^2} \ . \tag{5.31}$$

In fact the nuclear density is better described by a Woods–Saxon than by a Gaussian shape. While the Fourier transform of a Woods–Saxon distribution must be evaluated numerically, an alternative analytic form is virtually indistinguishable from it. [39] We consider a coordinate space density

$$\rho(\mathbf{r}) = \int d^3r' \rho_0(\mathbf{r}') \rho_1(\mathbf{r} - \mathbf{r}') \ , \tag{5.32}$$

where $\rho_0(\mathbf{r})$ is a constant within a sphere of radius $R_0 = (R^2 - 5s^2)^{1/2}$ and zero outside, $\rho_1(\mathbf{r}) = e^{[-\frac{1}{2}(r/s)^2]}$, and $s \approx 1$ fm. The Fourier transform of this density, which physically represents a nearly constant interior and a surface of thickness s, is given by

$$F_b(q) = \frac{3j_1(qR_0)}{qR_0} e^{-\frac{1}{2}(qs)^2} \ . \tag{5.33}$$

In Fig. 5, we compare the squares of the form factors $F_a(q)$ and $F_b(q)$ for ^{131}Xe. For this system, the radius is roughly $R \approx 6.1$ fm ≈ 31 GeV^{-1}. Deviations start to show up for $q \approx 0.1$ GeV, for which $qR \approx 0.3$. Similar results also obtain in ^{93}Nb and are suggested in other nuclei by the work of Ref. 29. In general, differences between the two form factors should be small enough that either will suffice for determining count rates in low-threshold detectors.

6. Spin–Dependent Neutralino Elastic Scattering

6.1. *The single-particle model*

The earliest calculations of axial or spin–dependent [40,41] elastic scattering of galactic dark matter utilized an extreme single-particle model (SPM) to describe the target nucleus the basic assumption is that nucleons pair off to zero angular momentum

(and zero spin). In an odd-mass nucleus, then, the total nuclear spin arises from the single remaining unpaired particle. For an unpaired nucleon in a single-particle orbit with quantum numbers (nlj), the expectation value of the spin operator $\hat{S}_z$ in the state with $m = j$ is given (in units of $\hbar$) by

$$S = \langle nljm = j | \hat{S}_z | nljm = j \rangle = \frac{j(j+1) - l(l+1) + \frac{3}{4}}{2j+2} . \tag{6.34}$$

This $m = j$ expectation value is related to the reduced matrix element used earlier by

$$\langle nljm = j | \hat{S}_z | nljm = j \rangle = \frac{(j\ 1\ j\ 0\ |\ j\ j)}{\sqrt{2j+1}} \langle nlj \| \hat{S} \| nlj \rangle . \tag{6.35}$$

At finite momentum transfer, we need to know how the spin is distributed over the nucleus. In the SPM, the distribution is determined solely by the radial wave function of the unpaired nucleon.

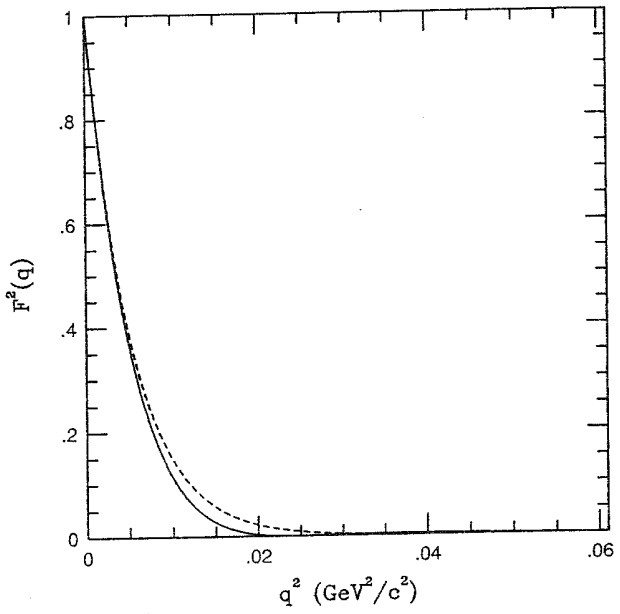

Fig. 5. Squares of the spin–independent form factors F_a (dashed line) and F_b (solid line) versus q^2 for ^{131}Xe.

Unfortunately, the SPM is not appropriate for most nuclei. In many odd-mass nuclei away from closed shells, it does not even correctly predict the ground state angular momentum. In nuclei with a single particle or hole relative to a doubly magic core, the SPM reproduces the angular momenta and parities of the lowest levels but does not quantitatively reproduce other more detailed properties, among these

magnetic dipole moments and transitions. The magnetic dipole or M1 operator can be expressed as

$$\hat{\mu} = \hat{\mu}_p + \hat{\mu}_n = \sum_{\rho=p,n} (g_\rho^l \hat{L}_\rho + g_\rho^s \hat{S}_\rho) \ , \tag{6.36}$$

where $\hat{L}$ is the orbital angular momentum operator and the "g-factors" are given (in nuclear magnetons) by $g_p^l = 1$, $g_p^s = 5.586$, $g_n^l = 0$, and $g_n^s = -3.826$. The M1 operator is clearly related to the spin operators of relevance to dark matter detection. The magnetic moments that arise in the extreme single-particle model are referred to as Schmidt moments. A survey of data in comparison with Schmidt values is given in Ref. 42. Even for nuclei with only a single particle or hole outside a doubly-magic core these values are not perfect and the discrepancies are much more pronounced away from closed shells. Many effects are now known to modify the Schmidt predictions.[42] In nuclei in which the closed core is not spin saturated, M1 polarization of the core by the odd particle plays a significant role. Away from closed shells, core–polarization effects are supplemented by configuration mixing within the valence space. And finally, at some level meson exchange currents also contribute.

In the sections to follow, we discuss several ways of incorporating these effects into calculations of the total proton and neutron spin, and of the associated finite-q form factors. As we will see, phenomenological approaches give fairly reliable information on the spin but are unable to describe the finite momentum response. Microscopic calculations, on the other hand, provide information at all relevant momentum transfers but are considerably more involved.

6.2. *The odd group model*

The simplest way to determine nuclear properties is through expeditious use of related experimental data. The Odd Group Model (OGM) is a version of this approach that is useful in odd-mass nuclei. Originally introduced in Ref. 43 in the context of magnetic moment data, it was subsequently expanded upon in Refs. 44 and 45. The authors of Ref. 46 adapted this analysis to determine the matrix elements governing q=0 neutralino spin–dependent scattering. For the purposes of this discussion, the basic assumption of the OGM is that in an odd-mass nucleus, containing an even number of one type of nucleon and an odd number of the other, the even group does not contribute to either the nuclear orbital or spin angular momentum. The structure of the odd group, which does contribute, is not defined in detail; rather, its properties are fit to known data.

To see how this works, consider the magnetic moment operator, Eq. (6.36), which can be rewritten in terms of operators and coefficients referring to the odd group (subscript o) and the even group (subscript e) according to

$$\hat{\mu} = g_o^l \hat{J} + (g_o^s - g_o^l)\hat{S}_o + (g_e^l - g_o^l)\hat{J}_e + (g_e^s - g_e^l)\hat{S}_e \ . \tag{6.37}$$

Neglecting the even group, we can express the expectation value of $\hat{\mu}$ (in the state with $M = J$) as

$$\mu = g_o^l J + (g_o^s - g_o^l) S_o \ , \tag{6.38}$$

so that

$$S_o = \frac{\mu - g_o^l J}{g_o^s - g_o^l} \ . \tag{6.39}$$

In other words, the magnetic moment of the system, its total angular momentum, and the g-factors, under the assumptions adopted, determine the spin matrix element of the odd group and thus of the entire nucleus.

This is clearly an improvement over the SPM. There it was assumed not only that the even group does not contribute but also that only the last nucleon of the odd group contributes. The OGM relaxes the latter assumption, asserting instead that the odd group must give the experimental magnetic moment. In Table 1 we compare the results obtained in the SPM and the OGM for some odd-mass nuclei, most of which are of potential importance to dark matter detection. Clearly there are substantial differences. In ^{29}Si the difference is more than a factor of three, which translates roughly into an order of magnitude difference in the elastic scattering cross section. These results illustrate the importance of correlation effects in the nuclear-spin matrix elements; knowledge of such large factors are essential for attempts to interpret dark-matter experiments.

Table 1. The spin content of several candidate detector nuclei based on the Odd Group Model.[46] In parentheses are given the corresponding results of the extreme Single-Particle Model.

	S_p	S_n
^{19}F	0.46 (0.50)	0 (0)
^{35}Cl	−0.15 (−0.30)	0 (0)
^{93}Nb	0.36 (0.50)	0 (0)
^{29}Si	0 (0)	0.15 (0.50)
^{73}Ge	0 (0)	0.23 (0.50)

At first glance, it would seem that a major weakness of the model is that it ignores neutron-proton correlations or equivalently, the role of the even system. To some extent this objection is valid; not all nuclear properties can possibly be well described. Reference 44 argues, however, that for odd-multipole operators like the spin, the even system is not overly important. The ground state contains admixtures with $J_e = 0$ through some $J_{\max}$. The $J_e = 0$ component is usually the largest, followed in size by those with $J_e = 2, 4, 6, \ldots$. An odd-multipole operator can mix the higher even angular momenta with the $J_e = 0$ component

only in second order. For this reason, although the OGM may not work well for even-multipole operators like the electric quadrupole moment, its assumption that the primary renormalization to the single-particle spin comes from the odd group should be reasonably valid. Of course, this argument breaks down if the dominant component of the ground state wave function is not $J_e = 0$. In highly collective nuclei and in particular those that are well deformed, the model may therefore not be as effective, a point to which we will return later.

In some nuclei it is possible because of the existence of additional data to relax the assumption that the even group does not contribute. Pairs of mirror nuclei (related to one another solely by the interchange of protons and neutrons) with $Z = N \pm 1$ provide what we need. For each pair, three relevant pieces of data exist: magnetic moments in each of the two nuclei and the Gamow–Teller beta decay from one to the other. The ft-value for the GT decay is related to other quantities by[45]

$$R^2(S_o - S_e)^2 = \left[\frac{6170}{ft} - 1\right] \frac{J}{J+1} , \tag{6.40}$$

where $R = g_A/g_V$ is the ratio of the axial-vector to the vector weak-interaction coupling coefficients. To determine S_o and S_e, we must include information from the magnetic moments as well. One weakness of the OGM is that it ignores pion-exchange contributions to these quantities. Since pion-exchange is an isovector process, we can legitimately avoid considering it by using the isoscalar magnetic moment

$$\mu_{IS} \equiv \mu_{Z,N} + \mu_{N,Z} = J + 0.76(S_o + S_e) + \mu_X , \tag{6.41}$$

where μ_X is the contribution from the exchange of heavy isoscalar mesons, which is known to be small[47,48] and can be estimated theoretically.[48] Since the quantity J_e is absent from the isoscalar sum, the two equations Eqs. (6.40) and (6.41) together contain (assuming that the effect of μ_X can be reasonably estimated) only the desired quantities S_o and S_e along with the ratio R, which we must somehow specify. The renormalization of this quantity in the nuclear medium has long been a subject of controversy. Two commonly used choices for R are its free-space value, 1.25 and 1.00, a number which arises in a number of different analyses,[42] most notably for our purposes a fit to magnetic moments and Gamow–Teller decays in Ref. 45. Once R has been fixed, we can solve the two equations for S_o and S_e. In Table 2, we summarize the results for several important nuclei with mirror partners for both choices of R. [We refer to this method as the Extended Odd Group Model (EOGM)]. Our prejudice, we should note, is for $R = 1.00$. In all the cases considered, the odd group indeed carries most of the spin (as expected) and the renormalization of the SPM results is larger for the odd group than for the even group, which is also not surprising in view of earlier remarks.

With Tables 1 and 2 we can compare the OGM and EOGM results for those cases in which both exist. In ^{29}Si, there is a significant discrepancy (in absolute

terms — we discuss the small numbers in ^{35}Cl shortly) between the two. ^{29}Si is one of the more highly collective nuclei in the sd shell, and correlations in the even group apparently play a role. Overall, we conclude that the OGM provides a reasonable approximation to the spin content of nuclei that are relatively light and also not too collective. The EOGM seems a quite accurate treatment wherever it can be applied.

Table 2. The spin content of several stable mirror nuclei of potential relevance to dark matter detection, evaluated using the EOGM.[46]

	S_p		S_n	
	$R = 1.00$	$R = 1.25$	$R = 1.00$	$R = 1.25$
^{19}F	0.415	0.368	−0.047	−0.001
^{35}Cl	−0.094	−0.083	0.014	0.004
^{29}Si	0.054	0.069	0.204	0.189

Both of these methods, however, suffer from the fact that they provide information for neutralino scattering only at $q = 0$. In light nuclei nothing else is necessary but in heavier nuclei we need to know the spin distribution. It is difficult to imagine how one might extend these phenomenological methods to higher q. Form factors from magnetic elastic electron scattering are an obvious idea but unfortunately the q-dependence of that process is quite different, making the extraction of neutralino form factors impossible. To treat heavy nuclei, we really need explicit calculations. We will present some of these after discussing analogous calculations in light nuclei, where high-q effects need not be considered.

6.3. *Shell-model calculations in light nuclei*

For all but the very lightest nuclei, the natural framework for microscopic calculations is the nuclear shell model. Shell-model technology has developed to the point that complete $0\hbar\omega$ calculations can now be carried out for all nuclei through the sd shell[49] and even for some in the fp shell.[50] For most heavier nuclei, however, further truncation is required, limiting the usefulness of the method.

Here we will describe shell-model calculations for several promising dark-matter detector candidates in the sd shell. Though the calculations are as complete as is currently possible, several approximations and assumptions nevertheless appear. Excitations from the doubly-magic ^{16}O core and excitations into higher major shells are treated implicitly in terms of effective interactions and effective operators that are not perfectly determined. Nonetheless, a wide variety of nuclear properties have been calculated in this region with impressive success.[49]

Shell-model calculations of the proton and neutron spin (for the explicit purpose of evaluating neutralino cross sections) were carried out in Ref. 51 in a number of

p-shell and sd-shell nuclei. The authors assumed an effective shell-model interaction that was derived from a Reid soft-core nucleon–nucleon potential. In general, the results are in good agreement with those of the EOGM. We present in Table 3 the calculated spin content of two representative nuclei, ^{19}F and ^{35}Cl. In ^{19}F, the calculations agree quite well with the EOGM results, an outcome that is not unexpected because the role of correlations is relatively small.

Table 3. The spin content of ^{19}F and ^{35}Cl from the shell-model calculations of Ref. 51, in comparison with the results of phenomenological EOGM calculations, assuming $R = 1.00$.

	Shell Model	EOGM
^{19}F		
neutrons	−0.109	−0.047
protons	0.441	0.415
^{35}Cl		
neutrons	−0.011	0.014
protons	−0.059	−0.094

In ^{35}Cl, correlations clearly are more important. They strongly suppress the proton spin, from a single-particle value of $S_p = -0.3$ to a correlated value quite close to zero. The precise number differs in the two approaches but the agreement is still good considering the amount of deviation from the single-particle results.

Reference 51 makes no predictions in ^{29}Si, a promising dark-matter detector element. In Ref. 52 however, the spin content of this isotope was calculated for reasons entirely unrelated to dark matter searches (the question addressed was "Where is the spin in ^{29}Si?"). These calculations used the Wildenthal USD interaction,[53] which has been tested in nuclei throughout the sd shell and is generally thought to be the best effective interaction currently available. The results for the spin content of ^{29}Si are summarized in Table 4, in comparison with those of the EOGM. (The OGM and SPM results for ^{19}Fl, ^{35}Cl and ^{29}Si can be found in Table 1.) As in ^{35}Cl, correlation effects play a major role in suppressing the spin content of the odd group. Here, there is some nonnegligible discrepancy between the shell-model and EOGM results, though the agreement is still reasonable considered alongside the single-particle value. Given the physics that is left out of the shell-model calculations, our prejudice is that the EOGM result is probably somewhat more accurate, though this statement cannot be made with any certainty.

In summary, the total spin content of the nucleus, which for light targets determines the axial-current neutralino cross section, can be obtained fairly reliably by any of several methods. Heavy nuclei, to which we now turn, are more complicated and the methods used to address them will necessarily be more involved.

Table 4. The spin content of ^{29}Si from the calculations of Ref. 49, in comparison with the results of phenomenological EOGM calculations, assuming $R = 1.00$.

	Shell Model	EOGM
neutrons	0.134	0.204
protons	−0.002	0.054

6.4. *Spin-dependent scattering from heavy nuclei*

The formalism associated with the evaluation of neutralino cross sections at the nonzero values of momentum transfer that occur in collisions with heavy nuclei was developed in Sec. 4. As noted earlier, we cannot extract the required information directly from experiment and thus must resort to detailed microscopic calculations. An approximation used in Ref. 29, in which single-particle form factors are scaled by the ratio of the OGM to SPM results at $q = 0$, while providing some qualitative insight, is usually not sufficiently accurate; as we shall show later, the form factor does not scale in general. In light nuclei the shell model is the method of choice and, fortuitously, a few heavy nuclei (for instance ^{93}Nb, which we will discuss shortly) have few enough valence particles to allow the same kind of treatment. Regrettably though, most heavy nuclei have too many valence particles for the shell model, as it currently stands, to handle without rather drastic truncations. Other methods for approximately treating the dynamics of heavy nuclei fall into a number of (often overlapping) classes, including:

(*i*) neutron–proton weak–coupling methods,[54]
(*ii*) symmetry–dictated truncation schemes,[55]
(*iii*) mean–field methods,[56]
(*iv*) quasiparticle methods,[56] and
(*v*) boson approximations.[57,58]

All provide a way to incorporate some of the important shell-model correlations. Unfortunately, none can be applied generically to the wide variety of behavior exhibited by heavy nuclei, ranging from vibrations, to rotations, to transitional behavior, to octupole deformation, etc.

We will describe three very distinct sets of calculations for the spin response of selected heavy nuclei. The first two focus on the properties of the candidate detector nuclei ^{131}Xe and ^{93}Nb. In Xenon we describe a quasiparticle Tamm–Dancoff Approximation (QTDA),[59] and in Niobium discuss a shell-model-type calculation.[60] The third set of calculations[61] uses boson approximation methods to estimate the effects of correlations on the spin content of collective nuclei throughout the periodic table. The method as currently implemented, however, provides no information on the distribution of spin required to evaluate cross sections at nonzero q.

A. ^{131}Xe

The spin response of a proposed ^{131}Xe scintillation chamber[36] was addressed in Ref. 59. The nucleus ^{131}Xe has 54 protons and 77 neutrons and is to a good approximation a spherical system dominated by pairing correlations. A natural way to describe pairing is through the BCS approximation. In such a treatment, the paired odd-A ground state is represented as a single quasiparticle built on a fully-paired zero-quasiparticle (0qp) even–even core. In ^{131}Xe, the relevant 1qp state can be expressed as $\nu^\dagger_{d_{3/2}}|\tilde{0}\rangle$, where $\nu^\dagger_{d_{3/2}}$ creates a neutron quasiparticle in the dominant $2d_{3/2}$ orbit and $|\tilde{0}\rangle$ represents the quasiparticle vacuum of the even–even core.

To the extent that additional correlations contribute to the ground state they should do so predominantly in the form of 3qp admixtures, of which there are two types

$$\left[\nu^\dagger_{d_{3/2}}[\nu^\dagger_k\nu^\dagger_l]^K\right]^{3/2}|\tilde{0}\rangle \ , \qquad \left[\nu^\dagger_{d_{3/2}}[\pi^\dagger_k\pi^\dagger_l]^K\right]^{3/2}|\tilde{0}\rangle \ . \tag{6.42}$$

The first involves a two-quasineutron excitation and the second a two-quasiproton excitation.

In even–even systems, two-quasiparticle excitations do not mix with the lowest order 0qp state; this fact follows directly from the BCS condition[56] that $H^{20} = H^{02} = 0$. In odd-mass nuclei, however, mixing can occur, through nonzero terms in the quasiparticle Hamiltonian like H^{13} or H^{31}. Such mixing is responsible for the often strong suppression of magnetic dipole moments in spherical odd-mass nuclei and has also been shown[62] to suppress low-lying GT transitions from the nucleus ^{127}I. Indeed, the method used in Ref. 59 for ^{131}Xe was borrowed with minor changes from an earlier analysis[62] of the GT response of ^{127}I to solar neutrinos.

To fully specify this kind of calculation, it is necessary to define an active set of orbits and a Hamiltonian. The calculations assumed a Z=40, N=40 core and included as active all the orbits in the 2s, 1d, 0g, and 0h single-particle levels. An effective Hamiltonian has two ingredients: a two-body effective interaction and effective single-particle energies. Single-particle energies were chosen from Ref. 63 and the effective interaction matrix elements from an analytic parametrization of the Paris-potential G matrix,[64] which was then subjected to two modifications. First, all neutron-proton monopole components of the effective interaction were replaced by their average value, so as to avoid an implicit effect on spherical single-particle energies. Second, all alike-nucleon pairing matrix elements were renormalized (as in Ref. 62) to guarantee the reproduction of experimental pairing gaps.

The mixing of 3qp components into the predominantly 1qp ground state was treated in perturbation theory. The amplitudes of admixed 3qp components in the ground state wave function turned out to be very small (typically less than about 0.05), justifying the perturbative treatment. The effect of the small admixtures on

the magnetic moment and spin was nonetheless significant. In the 1qp configuration, both the magnetic moment and the spin matrix elements reduce to the extreme SPM results: $\mu_{1qp} = 1.146$ nm (assuming free-nucleon g-factors), $S_n^{1qp} = -0.3$ and $S_p^{1qp} = 0$. When the small 3qp admixtures were included, the results were $\mu_{1qp+3qp} = 0.70$ nm and $S_n^{1qp+3qp} = -0.236$ and $S_p^{1qp+3qp} = -0.041$. It is reassuring that the calculations so accurately reproduced the quenching of the magnetic moment, which experimentally is 0.69 nm. The agreement suggests that the model space and the effective Hamiltonian were reasonable and lends credence to the spin predictions.

It is interesting to compare these results with those of the Odd Group Model. There, one finds that $S_n^{OGM} = -0.18$ and $S_p^{OGM} = 0$. The two methods lead to similar results, although as expected, the microscopic calculations permit a nonzero (albeit small) spin for the protons.

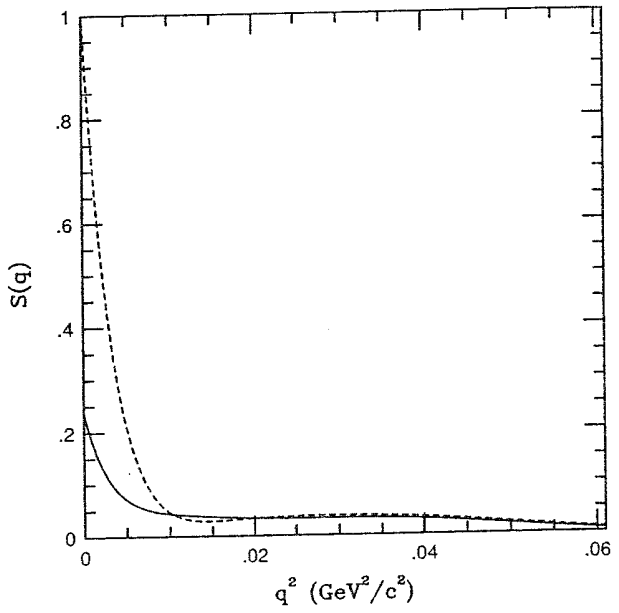

Fig. 6. The axial structure function S_A versus q^2 for a pure $\tilde{B}$ on ^{131}Xe. The dashed line is the prediction of the single-particle model; the solid line is the full result. The results are normalized for convenience so that single-particle curve goes to 1 at $q^2 = 0$.

In Fig. 6, we present the axial form factor $S_A(q)$ assuming that the neutralino is a pure $\tilde{B}$ ($a_0/a_1 = 0.31$). We also include for comparison the pure SPM result (both assume harmonic oscillator single-particle radial wave functions). The large difference at small values of q reflects the role of 3qp admixtures in determining the total spin. However, by a momentum transfer of $q^2 \approx 0.01$ GeV^2, the effect of correlations is washed out and the full results are virtually indistinguishable from the single-particle estimates. The reason is that, because of the oscillations in the

radial wave functions, the correlations no longer contribute coherently and the size of the deviation reflects the amount of 3qp admixing, which, as we have already remarked, is quite small.

B. ^{93}Nb

Reference 60 presents results for the response of a proposed ^{93}Nb detector.[37] The nucleus ^{93}Nb has Z=41 and N=52 and thus is only a few particles from doubly-magic ^{88}Sr. As such, it should not exhibit any pronounced collective behavior and should be amenable to a relatively complete shell-model treatment.

A complete $0\hbar\omega$ calculation, like those in the sd shell, would involve three valence protons distributed in all possible ways over the orbits of the Z=38-50 shell and two valence neutrons distributed over the the N=50-82 shell. While this model space provides a fairly realistic description of many of the properties of ^{93}Nb, the spin is not one of them. A proper description requires the inclusion of the spin polarization of the core. Its effects are far less significant in light nuclei, where the relevant cores (^{16}O or ^{40}Ca) are spin saturated. In heavy nuclei, the spin-orbit partners of high l orbits are split into different major shells and spin-flip excitations from the doubly-magic cores are possible. In the case of a ^{88}Sr core, for example, neutron excitations from the (filled) $0g_{9/2}$ orbit to the (empty) $0g_{7/2}$ orbit are possible and even if admixed very weakly can contribute significantly to spin-dependent properties.

With these facts in mind, the authors of Ref. 60 calculated the Niobium spin-response in two stages. First, a relatively small-space shell-model calculation was performed; subsequently, polarization effects from a much larger space were estimated. The small shell-model space, which consisted of a total of 20 $J^\pi = \frac{9}{2}^+$ states, was constructed by assuming an inert ^{88}Sr core and distributing the three valence protons over the $1p_{1/2}$ and $0g_{9/2}$ orbits and the two valence neutrons over the $1d_{5/2}$ orbit. The assumption that only a single valence neutron orbit is important was motivated by the existence of a fairly strong subshell gap at N=56 (Ref. 65). In this space, the shell-model Hamiltonian consisted of single-particle energies taken from the spectra of the single-particle and single-hole nuclei ^{89}Sr and ^{89}Y and a residual two-body surface-delta interaction (SDI), with isovector and isoscalar strength parameters $A_1 = 0.35$ MeV and $A_0 = 0.60$ MeV respectively. These SDI strengths were taken from Ref. 66, where they were found to accurately reproduce empirical matrix elements for this region of the periodic table. The resulting ground state magnetic moment (with free-nucleon g-factors) was $\mu = 6.36$ nm, significantly quenched relative to the SPM result of 6.79 but still somewhat larger than the experimental value of 6.17. It is apparent that a small shell-model space, while describing many properties of ^{93}Nb, does not incorporate the necessary correlations required to fully describe M1 data.

In the next stage, the shell-model basis was expanded to include all states in which one proton or one neutron was excited (either from one of the valence orbits

or from the $0g_{9/2}$ neutron core orbit) into any orbit of the sdg shell. The only such states that were not included were those in which a $0g_{9/2}$ neutron was excited into the $1d_{3/2}$ orbit. The resulting space consisted of roughly 2050 states with $J^\pi = \frac{9}{2}^+$. About 950 of these states were treated by diagonalization of the Hamiltonian matrix and the remainder in perturbation theory. The small-space SDI parameters were extended to the entire calculation, with the remaining single-particle energies extracted from additional experimental data on one-particle and one-hole nuclei. It should be noted that the SDI is usually not considered a good effective interaction when more than one valence shell for each type of particle is included; it was used, nevertheless, in the absence of a better prescription.

The net result of the full calculation was a magnetic moment of only 5.88 nm, which is somewhat smaller than the experimental value. A discrepancy in that direction, however, is not too bothersome; it is known[42] that meson-exchange currents can renormalize orbital proton g-factors upwards by about 10%, raising the calculated magnetic moments without affecting the spin. The full wave functions therefore appear reasonable for describing the spin properties of ^{93}Nb.

In Table 5, we present the full results for the total neutron and proton spins, alongside the small-space results and the those of the SPM and OGM approaches. Surprisingly, our best results are in closer agreement with the SPM predictions than those of the Odd Group Model. A detailed explanation of why this is so is given in Ref. 60. Essentially, the very large ground state angular momentum (9/2), combined with other features, makes ^{93}Nb a worst-case scenario for the OGM.

Table 5. The spin content of ^{93}Nb from the calculations of Ref. 60, in comparison with the SPM and OGM results.

	Shell Model		SPM	OGM
	Large Space	Small Space		
neutrons	0.08	0.04	0.0	0.0
protons	0.46	0.48	0.5	0.36

Except in such rare cases, the OGM is still preferable to the SPM since it incorporates at least approximately some correlation effects. Figure 7 shows the full axial structure function under the assumption of a nearly pure Higgsino (i.e. squark exchange is neglected) with $a_0/a_1 \approx 0.12$. As in the Xenon analysis, harmonic oscillator radial wave functions were used. Here the single-particle result differs significantly from the full structure function even at large q. The reason is that the SPM in Niobium is not a good starting point for perturbation theory; its place is taken in that regard by the small valence space. The small-space results approach the full results for large values of q, for the same reason the single-particle curve did in ^{131}Xe. It is only spin polarization of the core that dies off at large q.

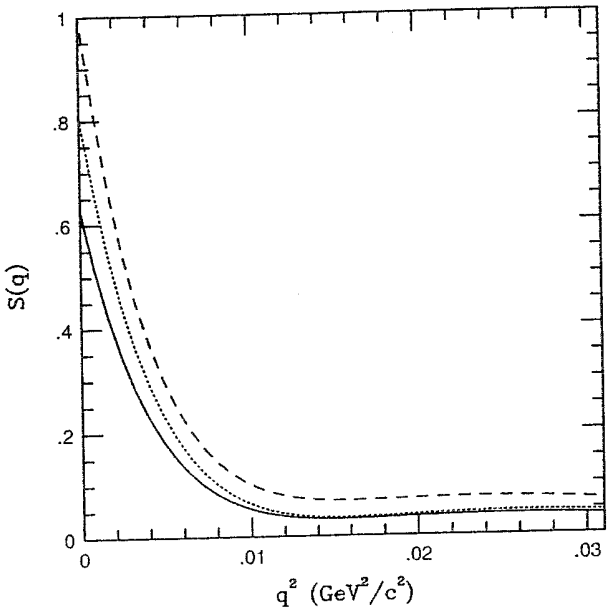

Fig. 7. The axial structure function S_A versus q^2 for a higgsino on ^{93}Nb. The dashed line is the prediction of the single-particle model, the dotted line is the small-space prediction, and the solid line is the full result. The normalization has again been adjusted so that the single-particle $S_A(0) = 1$.

In some sense, the results in ^{131}Xe and ^{93}Nb taken together are a bit disheartening. It would be nice to have a prescription to generate the form factors without doing complicated nuclear structure calculations. This would be possible if only one type of correlation effect, either core-polarization or valence-space configuration-mixing, were important. In the former case, one could use the OGM to estimate the $q = 0$ form factor and then simply match this smoothly to a large q form factor from the SPM. In the latter case, an overall scaling of the SPM form factor to agree at $q = 0$ with the OGM result, as has been proposed in Ref. 29, would be reasonable. In general, however, both types of correlations contribute and neither prescription is justified.

C. *IBFM calculations*

The heavy-nuclei calculations we have discussed so far are limited to nuclei near closed shells or to those in which pairing correlations dominate. When other collective features become prominent, an alternative approach must be employed. Reference 61 proposed the use of the Interacting Boson-Fermion Model as a method for estimating the spin content of odd-A nuclei with more-or-less arbitrary collective

correlations. This method is in some sense related to the phenomenology presented earlier but makes different assumptions about the structure of the wave functions. Through careful fits to data, it is able to obtain meaningful results for many nuclear properties. Like the other phenomenological methods we have discussed, however, it cannot in its current form give information on the spin response at finite q.

We will not go into detail on the Interacting Boson-Fermion Model, but simply refer the reader to a recent monograph.[58] Suffice it here to note that the model has been highly successful in describing a wide variety of low-lying collective features in odd-mass nuclei and that it is clearly founded in the nuclear shell model, although to date the details of this connection have not been elaborated for all types of collective behavior. The basic idea of the model is to describe the low-lying states of an odd-mass nucleus as an odd fermion coupled to an even–even core that is represented in terms of the neutron-proton Interacting Boson Model (IBM2).[57] When the fermion (representing the last valence nucleon) is included, the model is called IBFM2.

The IBM2 core is described in terms of s (L=0) and d (L=2) bosons for neutrons and protons separately. These bosons are meant to represent the lowest-energy correlated pairs of valence nucleons. Already we see that the model includes physics beyond the SPM or OGM, in that some collective pairs with nonzero angular momenta are included for both types of particles. The bosons are assumed to interact via a fairly simple Hamiltonian whose parameters (typically 5 or 6) are fit to the low-lying energy levels of the even–even (core) nucleus.

The coupled fermion is typically limited to a small number of single-particle orbits near the fermi surface and is assumed to interact with the core via a semi-microscopic core-particle interaction. Once the low-lying wave functions have been determined, other properties can be studied. This too however, requires assuming a structure for operators and determining their parameters by fits to data. For example, the magnetic dipole operator is usually represented as

$$\hat{T}(M1) = \hat{T}_B(M1) + \hat{T}_F(M1) \ , \tag{6.43}$$

where

$$\begin{aligned} \hat{T}_B(M1) &= \sqrt{\frac{3}{4\pi}}(g_\nu \hat{L}^B_\nu + g_\pi \hat{L}^B_\pi) \ , \\ \hat{T}_F(M1) &= \sqrt{\frac{3}{4\pi}} g_F \ \hat{J}_F \ . \end{aligned} \tag{6.44}$$

Here the operators with superscript B refer to the bosons and $\hat{J}_F$ is the angular momentum operator of the odd fermion. The boson g-factors, g_ν and g_π, are parameters that are obtained from fits to magnetic dipole moments and M1 transition matrix elements in the even-even system. The fermion g-factor, g_F, on the other hand, is usually chosen on the basis of a microscopic mapping procedure.

Within the standard prescription just given, the bosons by assumption carry no spin. Microscopic calculations[67] for the structure of the bosons suggest that this is only approximately true. Thus, Ref. 61 included a boson component to the spin, which was estimated via the microscopic calculations of Ref. 67. In our view, these numbers are a bit suspect, except in vibrational nuclei where the microscopic basis of the IBM2 is well founded. For this reason, it is reassuring that the bosonic contribution to the spin is fairly small. The principal effect of correlations is to permit the uncoupled fermion to be distributed over several orbits, leading to modifications of the spin expectation values. These points are summarized in Table 6, where we compare the IBFM and SPM results for the calculated spin. The IBFM columns separately give the spins of the odd fermion and the proton and neutron bosons of the core.

Table 6. The unquenched spin content of some dark matter detector nuclei calculated in the IBFM,61 in comparison with the corresponding SPM results. The labels $p(n)$ distinguish odd-proton from odd-neutron systems.

	p or n	$S_{p(n)}^{\mathrm{IBFM}}$	S_{π}^{IBFM}	S_{ν}^{IBFM}	$S_{p(n)}^{\mathrm{SPM}}$
^{73}Ge	n	0.469	−0.009	0.000	0.500
^{131}Xe	n	−0.280	0.000	0.003	−0.300

As noted earlier, the g-factors of the IBFM2 are determined by fits to M1 data and are invariably strongly quenched. Part of this quenching comes from spin polarization, which is not included in the IBFM, and part comes from nonnucleonic degrees of freedom. Simply renormalizing the spin to incorporate all sources of quenching leads to the results shown in Table 7. It should be noted that in Ref. 61, it is not the spin that is assumed to be quenched but rather the overall axial coupling constants that contribute to neutralino elastic scattering. However, for the purpose of this discussion the distinction is not important. In the end, the results are quite similar to those of the OGM, except for the few nuclei in which both kinds of bosons in the core carry a significant amount of spin. We reiterate that although the IBFM is designed to model heavy nuclei, it is not yet clear how to use it to calculate the finite-q response.

Table 7. The quenched spin content of some dark matter detector nuclei calculated in the IBFM.[61] The OGM results are included in parentheses for comparison.

	S_p	S_n
^{73}Ge	−0.005 (0)	0.245 (0.23)
^{131}Xe	0.000 (0)	−0.166 (−0.18)

D. *Still to be done:* ^{73}Ge

The most important remaining calculation is the full response of ^{73}Ge, the odd isotope in one of the most promising dark-matter detectors.[38] Estimates of the $q = 0$ response, in the OGM and the IBFM, are in reasonable accord (see Table 7). No method exists at present, however, for extending these results to nonzero q.

The IBFM method could in principle be used if it could explicitly incorporate the spin–polarization degree of freedom, perhaps by including three fermions (two of which represent a broken core pair) instead of just one. We are aware of some thoughts along these lines[68] and feel they should be pursued. Purely microscopic treatments of ^{73}Ge are exceedingly difficult. There is good evidence for coexistence between spherical and deformed shapes in this region, a situation that is too complicated for any of the methods that we have so far discussed. But, until a reliable calculation in ^{73}Ge has been carried out, the description of the nuclear physics of dark matter detection will be incomplete.

7. Prospects for Detection

We have just completed a detailed discussion of the nuclear physics in an area still fraught with uncertainties in the particle physics and the astrophysics. Why have we bothered? To some extent, the situation resembles that of neutrinoless double-beta decay. The neutrino may well have an effective mass many orders of magnitude less than an electron volt and there may be no right-handed currents, in which event neutrinoless double-beta decay will not be observed in the forseeable future. Nevertheless, knowledge of the nuclear matrix elements governing the process is essential. If no signal is seen, the nuclear physics allows limits to be placed on neutrino masses and right handed couplings. In the event that something is observed, it is needed to determine the values of these quantities.

The same is true here. There exist a variety of neutralino models, the parameters of which are not currently well constrained. Direct–detection searches may fail to see dark matter but without understanding neutralino–nucleus interactions, we will be able to deduce very little from that. And if a signal is seen, the nuclear physics is essential for deciding what kind of particle has been observed, whether its density is sufficient to account for the dark matter, etc.

Characteristics of the new detectors are obviously important considerations in assessing the likelihood of actually seeing neutralino dark matter. A recent discussion of detector technologies, thresholds, backgrounds, etc. appears in Ref. 2. Here we will look in a cursory way at expected event rates in detectors made from some of the elements we have considered earlier, disregarding complications due to background. The rates obviously depend on the SUSY parameters discussed in Sec. 3, which determine the mass and composition of the lightest neutralino, as well as on Higgs and squark masses. A complete analysis, examining all possibilities for these parameters, can result in rates that vary by several orders of magnitude

for a given detector type. Moreover, the simplest supersymmetric extension of the Standard Model can be modified so that event rates go up or down even more. For these reasons, it will be difficult to completely rule out supersymmetric dark matter, even with detectors that may be sensitive to a few events per month or year. We shall illustrate below, however, that over a range of supersymmetry parameter space, events do become frequent enough to be counted.

The total event rate per kilogram of material, assuming a Maxwellian distribution of velocities, is given by

$$R = 4\pi N(\pi\overline{v}^2)^{-3/2}\frac{\rho}{M_\chi}\int dv\ v^3\ \exp\left(-\frac{v^2}{\overline{v}^2}\right)\ \int_{2M_A\kappa}^{4M_R^2v^2} dq^2\ \frac{d\sigma}{dq^2}\ , \tag{7.45}$$

where $N = 6.02 \times 10^{26}/A$, $\overline{v} \approx .001c$ is the mean neutralino velocity, $\rho \approx 0.4$ GeV/cm^3 is the neutralino density, κ is the detector threshold, M_A is the mass of the nucleus, and M_R is the reduced neutralino-nucleus mass. To keep matters simple we have neglected the motion of the earth around the sun; the resulting annual variation in flux may in fact provide an important dark-matter signal.[34] We have also neglected the motion of the sun in the galactic plane. In some of the proposed detectors, the direction of recoil may be measurable and an asymmetry in this quantity could constitute another neutralino signal. The shape of the recoil spectrum will also be a useful characteristic.

Using the relation $T = \frac{q^2}{2M_A}$ and combining Eq. (4.24) with Eq. (7.45), we have

$$\frac{dR}{dT} \propto [S_A(\sqrt{2M_AT}) + S_S(\sqrt{2M_AT})]\ \exp\left(-\frac{M_AT}{2M_R^2\overline{v}^2}\right)\ , \tag{7.46}$$

i.e. an additional exponential falloff due to the velocity distribution modifies the form-factor dependence we discussed earlier. To illustrate the range of expected count rates, we display contour plots of the event rate per month per kilogram of detector versus the supersymmetry parameters μ and M. Because we can think of no sensible way to show variation with the third parameter, $\tan\theta_v$ at the same time, we have fixed it somewhat arbitrarily at $\tan\theta_v = 8$. (We have also chosen the lightest Higgs mass to be 60 GeV and the squark masses to be $1.1M_\chi$.) For most of the plotted region, which represents a slice of available parameter space, the lightest neutralino has a mass greater than 50 GeV and the parameter Ω, according to the annihilation calculations of Ref. 17, is less than or equal to 1.

Figures 8 and 9 display contours of constant event rate for the spin–dependent and total response respectively in ^{19}F. Because this is a light nucleus, the spin-dependent response dominates. The figures clearly show that count rates vary by several orders of magnitude over the parameter space. It is difficult to imagine detecting .01 counts per month but 5 per month seems well within the range accessible to new detectors.

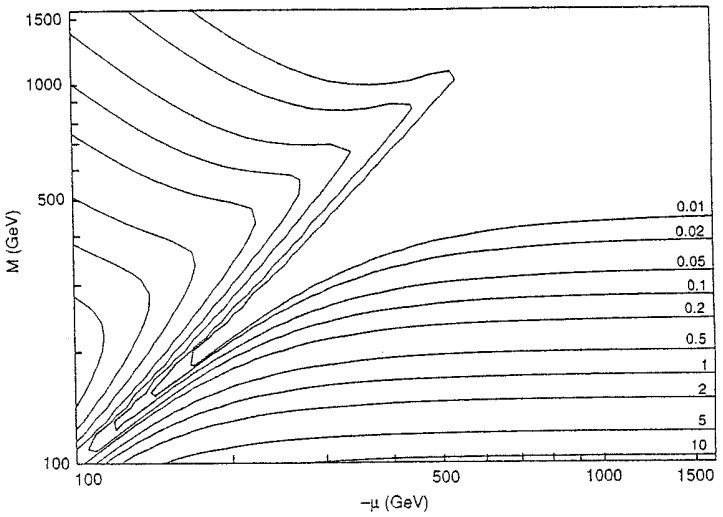

Fig. 8. Contours of constant count rate per month per kg of detector material (^{19}F) for the spin–dependent scattering of neutralinos versus the parameters μ and M (other parameters are specified in the text).

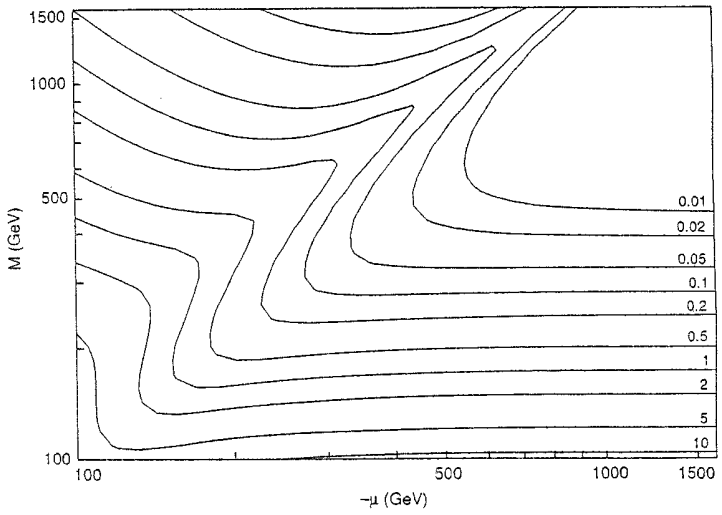

Fig. 9. Contours of constant count rate per month per kg of detector material (^{19}F) for the summed spin–dependent and spin–independent scattering of neutralinos versus the parameters μ and M.

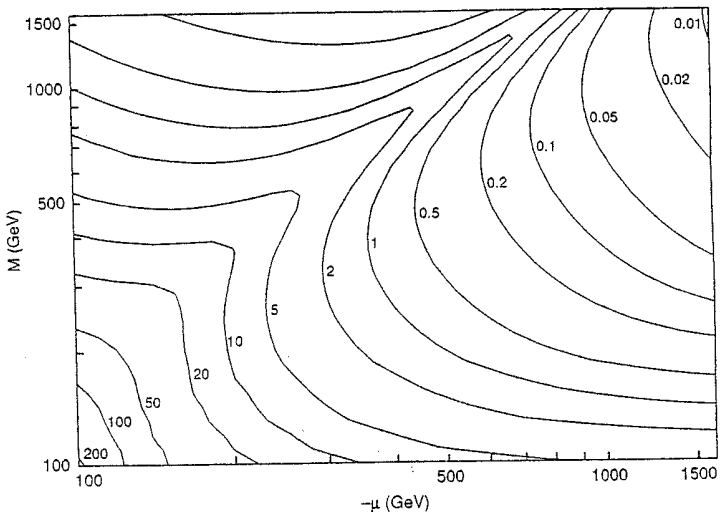

Fig. 10. Contours of constant count rate per month per kg of detector material (^{93}Nb) for the summed spin–dependent and spin–independent scattering of neutralinos versus the parameters μ and M.

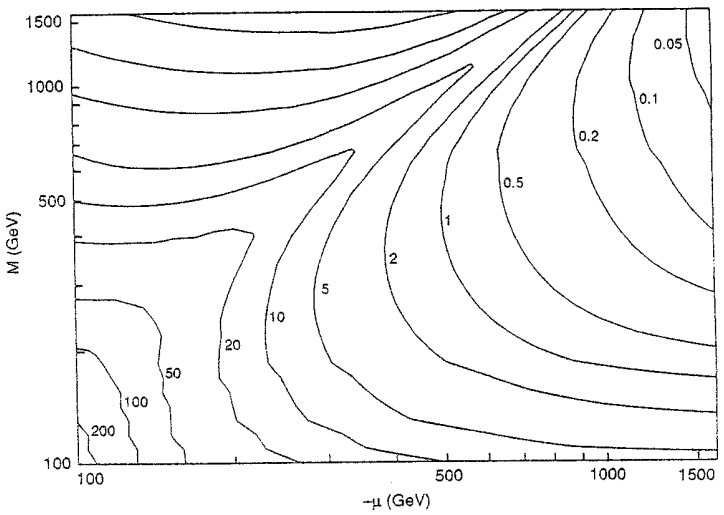

Fig. 11. Same as Fig. 10 except the reduction due to form factors is omitted.

Figures 10 and 11 present similar plots for Niobium. In this instance, we have shown separately the event rates with and without the form factors, the calculation of which we have described above. The net effect of the form factors is to shift the contours slightly, though in the upper right hand corner, where the neutralino

is very heavy, the effect is pronounced. In Niobium, a relatively heavy element, the spin–independent response is largest over most of the parameter space, and in the lower left corner it yields count rates larger than in Fluorine. Only when μ gets considerably bigger than M (i.e in the lower right hand corner of the figure, where the neutralino is essentially pure $\widetilde{B}$), is the spin–dependent response both substantially larger than the spin–independent response and large enough to be accessible to detectors.

These figures and others like them indicate that the new ultra-sensitive dark-matter detectors stand a reasonable chance of observing neutralinos, should they exist. Together with information to come from SSC or LHC, which will develop our knowledge of superparticle masses and other parameters in the superlagrangian, the nuclear physics presented here will allow us to extract information on the composition of the dark matter. Without this understanding the experimental results, no matter what they are, will be much harder to interpret.

Acknowledgments

We would like to thank David Seckel for generous help with parts of this manuscript and acknowledge useful conversations with F. Iachello and R. Flores. Two of the authors (JE and PV) acknowledge the hospitality of the Institute for Nuclear Theory in Seattle, where part of this work was conducted. We were supported in part by National Science Foundation under grant #PHY-9108011 and by the U.S. Department of Energy under Contract #DE-F603-88ER-40397.

References

1. J. R. Primack, D. Seckel and B. Sadoulet, *Ann. Rev. Nucl. Part. Sci.* **38**, 751 (1988).
2. P. F. Smith and J. D. Lewin, *Phys. Rep.* **187**, 203 (1990).
3. M. S. Turner, *Phys. Scripta* **T36**, 167 (1991).
4. See, e.g. *Dark Matter: XXIIIrd Rencontre de Moriond*, eds. J. Audouze and J. Tran Thanh Van (Editions Frontieres, Gif sur Yvette, 1988); *Low Temperature Detectors for Neutrinos and Dark Matter III* , eds. L. Brogiato et al. (Editions Frontieres, Gif sur Yvette, 1990); *Proc. Workshop Dark Matter and the Structure of the Universe*, ed. M. Sasaki (Hiroshima University, 1989).
5. S. Tremaine, *Physics Today* **Vol 45, No. 2**, 28 (1992).
6. T. P. Walker *et al. Ap. J.* **376**, 51 (1991).
7. S. Casetrono and T. S. van Albada, in *Baryonic Dark Matter*, eds. D. Lynded-Bell and G. Gilmore (Kluwer Academic, Dordrecht, 1990), pp. 237.
8. K. Griest, *Ap. J.* **366**, 412 (1991).
9. B. Paczynski, *Ap. J.* **301**, 1 (1986).
10. M. Spiro, in *Neutrino 90, Nucl. Phys.* **B19**, 234 (1991).
11. C. Alcock *et al.* in *Robotic Telescopes in the 1990's*, ed. A. V. Filipenko (ASP, San Francisco).
12. E. W. Kolb and M. S. Turner, *The Early Universe* (Addison-Wesley, Redwood City, CA, 1990).

13. L3 Collaboration, B. Adeva *et al. Phys. Lett.* **B231**, 509 (1989); ALEPH collaboration, D. Decamp *et al. Phys. Lett.* **B231**, 519 (1989) and **B235**, 399 (1990); OPAL collaboration, M. Z. Akrawy *et al. Phys. Lett.* **B231**, 530 (1989); DELPHI collaboration, P. Aarnio *et al. Phys. Lett.* **B231**, 539 (1989); MARK II collaboration, G. S. Abrams *et al. Phys. Rev. Lett.* **63**, 724 and 2173 (1989).
14. H. Goldberg, *Phys. Rev. Lett.* **50**, 1419 (1983).
15. J. Ellis, J. S. Hagelin, D. V. Nanopolous, K. Olive and M. Srednicki, *Nucl. Phys.* **B238**, 453 (1984).
16. H. E. Haber and G. L. Kane, *Phys. Rep.* **117**, 75 (1985).
17. K. A. Olive and M. Srednicki, *Phys. Lett.* **B230**, 78 (1989); K. Griest, M. Kamionkowski and M. S. Turner, *Phys. Rev.* **D41**, 3565 (1990).
18. L3 collaboration, B. Adeva *et al. Phys. Lett.* **B236**, 109 (1990); ALEPH collaboration, D. Decamp *et al. Phys. Lett.* **B236**, 86 (1990).
19. K. Griest, *Phys. Rev.* **D38**, 2357 (1988).
20. G. B. Gelmini, P. Gondolo and E. Roulet, *Nucl. Phys.* **B351**, 623 (1991).
21. R. Barbieri, M. Frigeni and G. F. Giudice, *Nucl. Phys.* **B313**, 725 (1989).
22. R. L. Jaffe and A. Manohar, *Nucl. Phys.* **B337**, 509 (1990).
23. J. Ashman *et al. Phys. Lett.* **B206**, 364 (1988); J. Ashman *et al. Nucl. Phys.* **B328**, 1 (1989).
24. G. Baum *et al. Phys. Rev. Lett.* **37**, 1261 (1976); G. Baum *et al. Phys. Rev. Lett.* **51**, 1135 (1983); G. Baum *et al. Phys. Rev. Lett.* **45**, 2000 (1980).
25. G. Karl, Guelph University preprint, 1991
26. R. Decker *et al. Nucl. Phys.* **A512**, 629 (1990).
27. J. Gasser, H. Leutwyler and M. E. Sainio, *Phys. Lett.* **B253**, 252 (1991).
28. M. Kamionkowski, *Phys. Rev.* **D44**, 3021 (1991).
29. J. Ellis and R. Flores, *Phys. Lett.* **B263**, 259 (1991)
30. M. Mori *et al. Phys. Lett.* **B270**, 89 (1991)
31. J. Ellis, R. A. Flores and J. D. Lewin, *Phys. Lett.* **B212**, 375 (1988).
32. J. D. Walecka, in *Muon Physics*, ed, V. W. Hughes and C. S. Wu (Academic, New York, 1975), Vol. 2, pp. 113.
33. S. P. Ahlen *et al. Phys. Lett.* **B195**, 603 (1987);
34. K. Freese, J. Frieman and A. Gould *Phys. Rev.* **D,**, 37 (193388)88.
35. B. A. Young *et al. Nucl. Inst. Meth.* **A311**, 195 (1992).
36. P. Belli *et al. Il Nuovo Cimento* **A103**, 767, 1990.
37. R. J. Gaitskell *et al. Physica* **B169**, 445 (1991).
38. B. Sadoulet, in *Proc. 4th Int. Conf. Low Tem. Dark Matter and Neutrinos*, ed. N. Booth (Oxford, September 1991) (to be published).
39. R. H. Helm, *Phys. Rev.* **104**, 1466 (1956).
40. M. W. Goodman and E. Witten, *Phys. Rev.* **D31**, 3059 (1985).
41. J. Ellis and R. A. Flores, *Nucl. Phys.* **B307**, 883 (1988).
42. See, e.g., B. Castel and I. Towner, *Modern Theories of Nuclear Moments*, (Clarendon Press, Oxford, 1990).
43. A. de Shalit, *Phys. Rev.* **91**, 83 (1953).
44. C. F. Clement and S. M. Perez, *Phys. Lett.* **B100**, 294 (1981)
45. B. Buck and S. M. Perez, *Phys. Rev. Lett.* **50**, 1975 (1983).
46. J. Engel and P. Vogel, *Phys. Rev.* **D40**, 3132 (1989).
47. I. S. Towner, *Phys. Rep.* **155**, 263 (1987).
48. S. Raman, C. A. Houser, T. A. Walkiewicz and I. S. Towner, *At. Data Nucl. Data Tables* **21**, 567 (1978).

49. B. A. Brown and B. H. Wildenthal, *Ann. Rev. of Nucl. and Part. Sci.* **38**, 29 (1988).
50. E. Caurier, A. Poves and A. P. Zuker, *Phys. Lett.* **B252**, 13 (1990).
51. A. F. Pacheco and D. D. Strottman, *Phys. Rev.* **D40**, 2131 (1989).
52. B. A. Brown, *Nucl. Phys.* **A522**, 221c (1991).
53. B. H. Wildenthal, *Progress in Particle and Nuclear Physics* **11**, 5 (1984).
54. See, e.g. W. Haxton and G. J. Stephenson Jr., *Prog. Part. Nucl. Phys.* **12**, 409 (1984); J. Engel, P. Vogel, X. Ji and S. Pittel, *Phys. Lett.* **B225**, 5 (1989).
55. See, e.g. X. Ji, M. Vallieres and P. Halse, *Phys. Lett.* **B197**, 484 (1987); X. Ji, B. H. Wildenthal and M. Vallieres, *Nucl. Phys.* **A492**, 215 (1989); O. Castaños and J. P. Draayer, *Nucl. Phys.* **A491**, 349 (1989).
56. See, e.g. P. Ring and R. Schuck, *The Nuclear Many Body Problem* (Springer Verlag, New York, 1980).
57. F. Iachello and A. Arima, *The Interacting Boson Model* (Cambridge University Press, Cambridge, 1991).
58. F. Iachello and P. Van Isacker, *The Interacting Boson-Fermion Model* (Cambridge University Press, Cambridge, 1991).
59. J. Engel, *Phys. Lett.* **B264**, 114 (1991).
60. J. Engel, S. Pittel, E. Ormand and P. Vogel, *Phys. Lett.* **B275**, 119 (1991).
61. F. Iachello, L. M. Krauss and G. Maino, *Phys. Lett.* **B254**, 220 (1991).
62. J. Engel, S. Pittel and P. Vogel, *Phys. Rev. Lett.* **67**, 426 (1991).
63. R. Madey, *et al. Phys. Rev.* **C40**, 540 (1989).
64. A. Hosaka, K. I. Kubo and K. Toki, *Nucl. Phys.* **A444**, 76 (1985).
65. C. M. Lederer and V. S. Shirley, eds. *Table of Isotopes, 6th edition*, (Wiley, New York, 1978).
66. P. Federman and S. Pittel, *Phys. Lett.* **B77**, 29 (1978).
67. M. Sambataro and A. E. L. Dieperink, *Phys. Lett.* **B107**, 249 (1981); M. Sambataro *et al. Nucl. Phys.* **A423**, 333 (1984).
68. F. Iachello and D. Vretenar, private communication.